

See discussions, stats, and author profiles for this publication at: <https://www.researchgate.net/publication/263957346>

# Effect of Stone Coal Chemical Composition on Sintering Behavior during Roasting

ARTICLE in INDUSTRIAL & ENGINEERING CHEMISTRY RESEARCH · DECEMBER 2013

Impact Factor: 2.59 · DOI: 10.1021/ie4022144

CITATIONS

3

READS

20

5 AUTHORS, INCLUDING:



Yunliang Zhao

Wuhan University of Technology

10 PUBLICATIONS 69 CITATIONS

SEE PROFILE



Shenxu Bao

Wuhan University of Technology

29 PUBLICATIONS 272 CITATIONS

SEE PROFILE



Tiejun Chen

Wuhan University of Science and Technology

11 PUBLICATIONS 77 CITATIONS

SEE PROFILE

# Effect of Stone Coal Chemical Composition on Sintering Behavior during Roasting

Yunliang Zhao,<sup>†</sup> Yimin Zhang,<sup>\*,†</sup> Shenxu Bao,<sup>†</sup> Tiejun Chen,<sup>‡</sup> and Xiang Liu<sup>†</sup>

<sup>†</sup>College of Resources and Environmental Engineering, Wuhan University of Technology, Wuhan 430070, People's Republic of China

<sup>‡</sup>College of Resources and Environmental Engineering, Wuhan University of Science and Technology, Wuhan 430081, People's Republic of China

**ABSTRACT:** During the roasting of stone coal, a sintering phenomenon usually occurs, which is related to the chemical composition of the stone coal. In this study, the sintering beginning temperature (SBT) and ash fusion temperatures (AFTs) of stone coal with different CaO, Fe<sub>2</sub>O<sub>3</sub>, SiO<sub>2</sub> and Al<sub>2</sub>O<sub>3</sub> content were investigated. FactSage has been used to calculate the phase distribution of roasted stone coal, to analyze how these components influence the sintering behavior during roasting. For stone coal with low CaO content, CaO reacted with albite, leucite, and quartz to generate an amorphous phase, which would easily cause sintering, while for stone coal with high CaO content, CaO took part in the formation of andradite and Na<sub>2</sub>Ca<sub>3</sub>Si<sub>6</sub>O<sub>16</sub>. Most Fe<sub>2</sub>O<sub>3</sub> in roasted stone coal stably existed as hematite in the system and did not react with others, which had almost no effect on sintering. SiO<sub>2</sub> and Al<sub>2</sub>O<sub>3</sub> in the stone coal contributed to hinder the formation of amorphous phases, especially for high Al<sub>2</sub>O<sub>3</sub> stone coal, in which mullite was generated.

## 1. INTRODUCTION

In China, stone coal is an important vanadium resource. The reserve of vanadium in stone coal accounts for more than 87% of the gross reserve of vanadium.<sup>1</sup> Therefore, much attention has been paid to investigate vanadium extraction from stone coal. Many technologies such as direct acid leaching, roasting-acid leaching, roasting-alkali leaching, calcified roasting-carbonate leaching, and low salt roasting-cyclic oxidation, have been proposed.<sup>2–5</sup>

However, most vanadium in stone coal exists as V<sup>3+</sup> replacing Al<sup>3+</sup> from a dioctahedral structure as isomorphism in mica group minerals.<sup>6,7</sup> To extract vanadium from stone coal, roasting with sodium additive at high temperature is usually necessary for breaking the crystal structure of aluminosilicate.<sup>8,9</sup> However, because most stone coal displays a high sensitivity to temperature, the sintering phenomenon during roasting usually occurs.<sup>10</sup> The sintering would lead to the enwrapment of vanadium and once vanadium is enwrapped, it could hardly be leached out.<sup>11</sup> On the other hand, rotary kilns have the advantages of high handling capacity and reliable operation<sup>12</sup> and are always used as the roasting equipment in the industry of extracting vanadium from stone coal. However, during the roasting of stone coal via rotary kiln, the sintering easily causes coating and ringing of the rotary kiln, which seriously hinders vanadium conversion and normal production.

Xu and Wang<sup>13</sup> researched the relationship between sintering and vanadium transformation during roasting of vanadium-bearing stone coal and discussed the sintering mechanism. Lu<sup>14</sup> investigated the effects of roasting temperature, additive species, and dosage on sintering during the roasting of stone coal. The roasting temperature, additive species, and dosage are the external factors that cause sintering. The internal factor is the chemical composition of the stone coal, and the reactions among different chemical components to generate the amorphous phase are the origin of the sintering. Because the

chemical composition is different from stone coal to stone coal,<sup>15</sup> the sintering behaviors during roasting of stone coal from different regions are also variable. However, to the best of our knowledge, the effect of stone coal chemical composition on sintering behavior during roasting has seldom been investigated.

In this work, sintering beginning temperatures (SBTs) and ash fusion temperatures (AFTs) of stone coal with different contents of CaO, Fe<sub>2</sub>O<sub>3</sub>, SiO<sub>2</sub>, and Al<sub>2</sub>O<sub>3</sub>, which are the main chemical components of stone coal in China,<sup>16</sup> were measured to investigate the effect of chemical composition on sintering during roasting. The thermochemistry software FactSage was used to calculate the phase distribution to analyze how these components influence the sintering behavior.

## 2. EXPERIMENTAL SECTION

**2.1. Materials.** A typical stone coal was collected from Hubei Province, China. The stone coal was first decarbonized at 700 °C for 1 h, and the decarbonized sample was used for roasting in this study. The mineral composition of the sample is given in Table 1; it is mainly composed of 54.36% SiO<sub>2</sub>, 10.59% Al<sub>2</sub>O<sub>3</sub>, 7.35% CaO, 5.93% Fe<sub>2</sub>O<sub>3</sub>, and 0.82% V<sub>2</sub>O<sub>5</sub>. In our previous research,<sup>17</sup> NaCl and Na<sub>2</sub>SO<sub>4</sub> were found to be the optimal roasting additives for vanadium extraction from stone coal. They were also used in this study, which were both analytical-grade and purchased from Tianjin Kemio Chemical Reagents, Ltd. CaO, Fe<sub>2</sub>O<sub>3</sub>, SiO<sub>2</sub>, and Al<sub>2</sub>O<sub>3</sub> (all analytical grade) were purchased from Sinopharm Chemical Reagent Corp.

**Received:** July 11, 2013

**Revised:** November 10, 2013

**Accepted:** December 9, 2013

**Published:** December 9, 2013

Table 1. Mineral Composition of Decarbonized Sample

mineral	formula	content (%)
quartz	SiO <sub>2</sub>	35
calcite	CaCO <sub>3</sub>	6
muscovite	KAl <sub>2</sub> (Si <sub>3</sub> AlO <sub>10</sub> )(OH) <sub>2</sub>	13
feldspar	KAlSi <sub>3</sub> O <sub>8</sub>	13
hematite	Fe <sub>2</sub> O <sub>3</sub>	11
kaolinite	(Al <sub>2</sub> O <sub>3</sub> )(SiO <sub>2</sub> ) <sub>2</sub> (H <sub>2</sub> O) <sub>2</sub>	5
silicates		4
sulfates		4
other		8

**2.2. Procedure and Test Method.** The decarbonized samples were mixed with 6% NaCl, 10% Na<sub>2</sub>SO<sub>4</sub>, and a certain content of the aforementioned oxides, and then they were ground to a particle size of <150 μm by a Model HLXZM-100 vibration mill. In the experiments, 3%, 6%, 9%, 12%, 15%, and 18% CaO, 3%, 6%, 9%, 12%, 15%, and 18% Fe<sub>2</sub>O<sub>3</sub>, 10%, 20%, 30%, and 40% SiO<sub>2</sub>, 5%, 10%, 15%, and 20% Al<sub>2</sub>O<sub>3</sub> were added, respectively. The mixture, which was made in a muffle furnace (Model SXZ-10-B), experienced three stages: heating (from room temperature to 850 °C, using a heating rate of 14 °C/min), roasting (850 °C for 2 h), and nature cooling (from 850 °C to 500 °C). When the temperature of the muffle furnace decreased to 500 °C, the roasted mixture was removed.

The mineral composition of the decarbonized sample was determined by quantitative evaluation of minerals scanning electronic microscopy (QEMSCAN). The apparent density of roasted sample was measured in accordance with Chinese standard GB/T 16913.3-1997. The apparent density was plotted as a function of roasting temperature. The temperature when the apparent density sharply increased was regarded as the SBT. The determination of AFTs was performed with HR-4A computer ash-melting point tester. The phase distribution of roasted stone coal was calculated by the thermodynamic software FactSage. Calculations were carried out in air atmosphere at a pressure of 1 atm. The formed phases with concentrations below 0.001 wt % were ignored.

### 3. RESULTS AND DISCUSSION

**3.1. Effect of CaO on Sintering Behavior.** During the roasting of stone coal, with increasing roasting temperature, volume shrinkage occurs and the apparent density of roasted sample increases.<sup>18</sup> When the temperature arrives at a certain value, the apparent density of roasted sample begins to increase significantly, and this temperature is regarded as the SBT. In the experiment, the apparent density of roasted samples, plotted as a function of roasting temperature with different CaO addition content, is provided in Figure 1. As shown in Figure 1, take 3% CaO addition content for example: in a roasting temperature range from 700 °C to 825 °C, the apparent density hardly changes, but when the temperature reaches 825 °C, there is a sharp increase in apparent density. Hence, for the samples with 3% CaO addition, the SBT is 825 °C. Similarly, the SBTs for samples with 6%, 9%, 12%, 15%, and 18% CaO addition are 800, 825, 850, 900, and 925 °C, respectively. Figure 2 shows the relationship between CaO addition content and SBT. With increasing CaO content, the SBT first decreases and then increases. The SBT reaches minimum at 6% CaO addition content. The effect of CaO addition content on the AFTs is given in Figure 3. The deformation temperature (DT), softening temperature (ST),

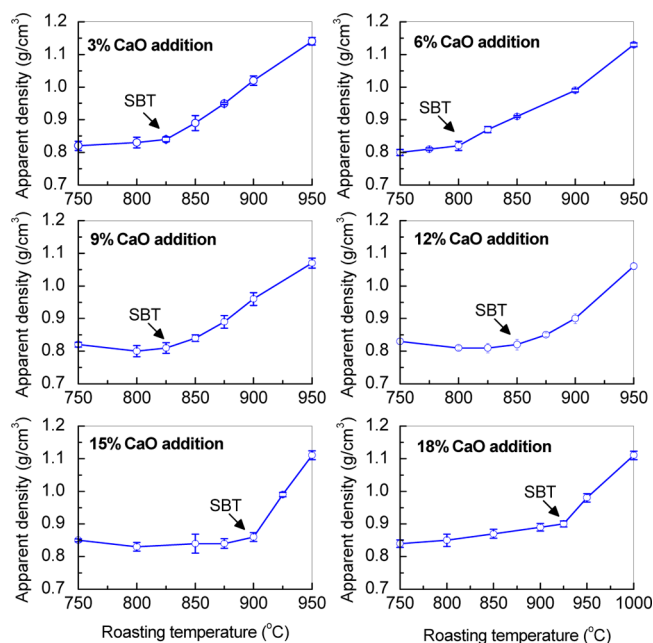


Figure 1. Apparent density against roasting temperature with different CaO addition content.

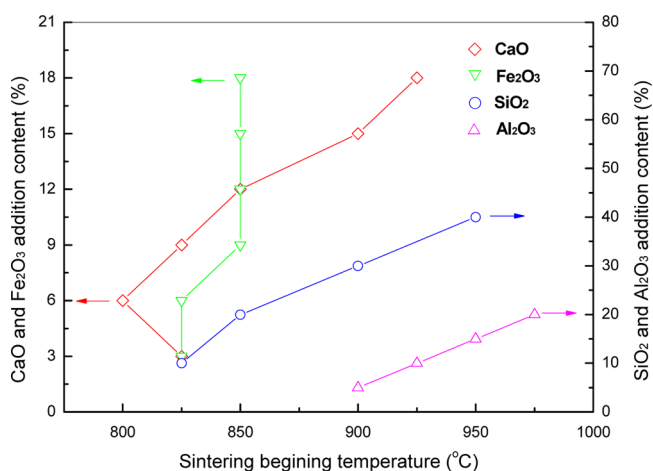


Figure 2. Effect of CaO, Fe<sub>2</sub>O<sub>3</sub>, SiO<sub>2</sub>, and Al<sub>2</sub>O<sub>3</sub> addition content on SBT.

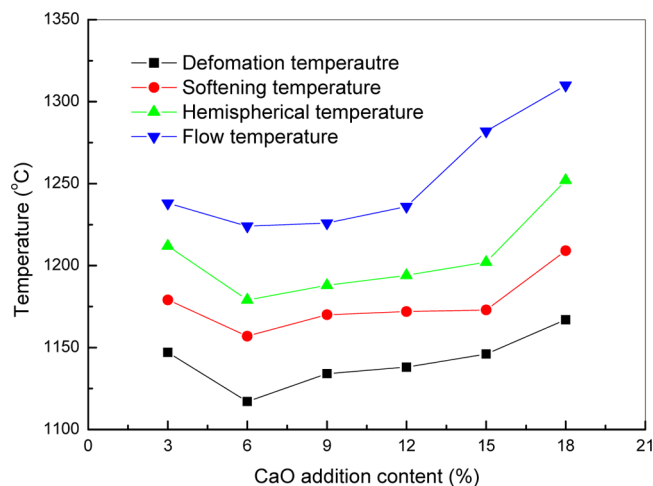


Figure 3. Effect of CaO addition content on AFTs.

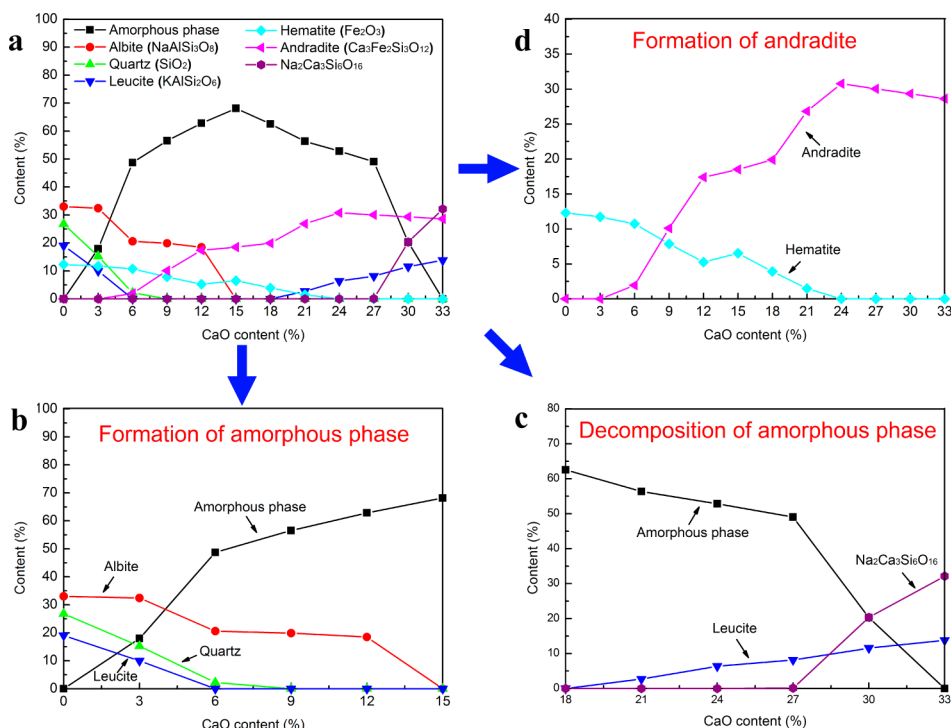


Figure 4. Phase distribution and reaction behavior as a function of CaO content calculated by FactSage.

hemispherical temperature (HT), and flow temperature (FT) drop as CaO content increase until the CaO addition content reaches 6%. The minimum AFTs occur at 6% CaO addition content, which is consistent with the SBT experiment. However, compared with SBT, the ST is much higher.

In order to illustrate why the SBT and AFTs vary with CaO content and the behavior of CaO influencing sintering during roasting, the phase distributions for the roasted samples with different CaO content are calculated by FactSage (see Figure 4). Because of the initial 7.35% CaO in the stone coal, for the stone coal with 3% and 18% CaO addition, the CaO content in the blend is actually 10.5% and 21.4%, respectively. As shown in Figure 4a, in the CaO content range of 10.5%–21.4%, the amorphous phase proportion has a maximum value, which means that, at this CaO content, the sample would be most easily sintered and has minimum SBT and AFT values. It agrees well with the fact that there are minimum values of SBT and AFTs in the experiment. In the CaO content range from 0% to 15%, it is observed that, as the CaO content increased, the albite, quartz, and leucite contents decrease, while the amorphous phase content increases significantly (Figure 4b). It is inferred that the amorphous phase is generated from albite, leucite, and quartz, and lime (CaO) also takes part in the reaction for the formation of amorphous phase. However, with further increases in CaO content (>15%), the amorphous phase content begins to decrease, while the eucite and Na<sub>2</sub>Ca<sub>3</sub>Si<sub>6</sub>O<sub>16</sub> contents increase (Figure 4c). It indicates that the amorphous phase decomposes into leucite and Na<sub>2</sub>Ca<sub>3</sub>Si<sub>6</sub>O<sub>16</sub>, and CaO is related to the decomposition. With increasing CaO content, the andradite content throughout increases and hematite content throughout decreases, it means lime (CaO) also participate in the reaction with hematite to generate andradite (Figure 4d). It is concluded that, for stone coal with low CaO content, CaO reacts with albite, leucite, and quartz to generate an amorphous phase, which would easily cause sintering during roasting, while

for stone coal with high CaO content, CaO takes part in the formation of andradite and Na<sub>2</sub>Ca<sub>3</sub>Si<sub>6</sub>O<sub>16</sub>.

**3.2. Effect of Fe<sub>2</sub>O<sub>3</sub> on Sintering Behavior.** The apparent density of roasted samples plotted as a function of roasting temperature with different Fe<sub>2</sub>O<sub>3</sub> addition content is presented in Figure 5. The SBTs for samples with 3%, 6%, 9%, 12%, 15%, and 18% Fe<sub>2</sub>O<sub>3</sub> addition are 825, 825, 850, 850, 850, and 850 °C, respectively (see Figure 5). With increasing Fe<sub>2</sub>O<sub>3</sub> content from 3% to 18%, the SBT only increase 25 °C (recall

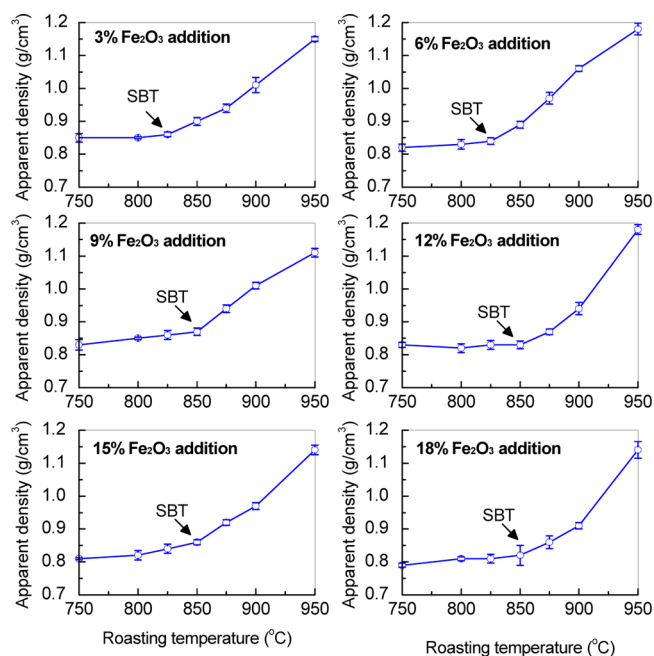


Figure 5. Apparent density against roasting temperature with different Fe<sub>2</sub>O<sub>3</sub> addition contents.

Figure 2). The  $\text{Fe}_2\text{O}_3$  content has little effect on the SBT. There are small changes on the DT, ST, HT, and FT, which are from 1153 °C to 1170 °C, from 1193 °C to 1227 °C, from 1224 °C to 1250 °C, and from 1254 °C to 1280 °C, respectively (Figure 6). The AFTs are also hardly affected by the changes of  $\text{Fe}_2\text{O}_3$  content.

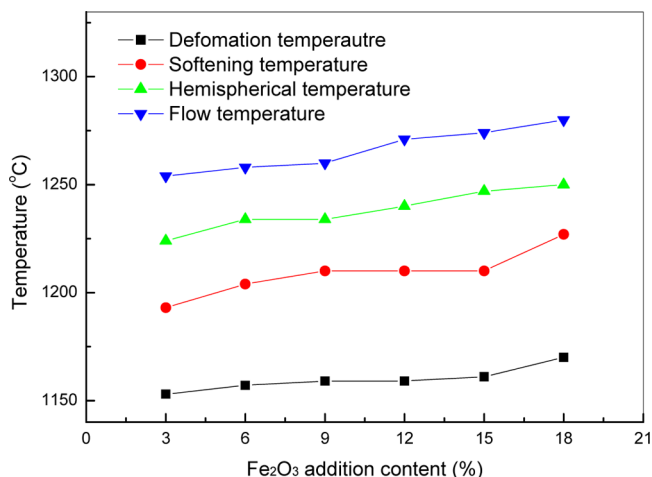


Figure 6. Effect of  $\text{Fe}_2\text{O}_3$  addition content on AFTs.

The phase distribution of roasted samples with different  $\text{Fe}_2\text{O}_3$  content calculated by FactSage is provided in Figure 7 to

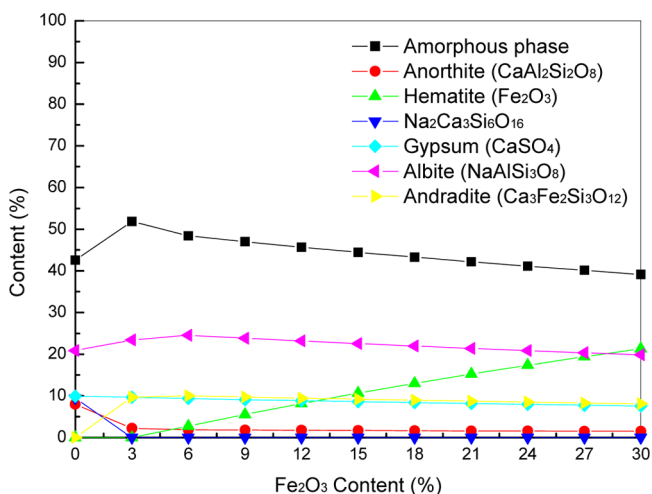


Figure 7. Phase distribution as a function of  $\text{Fe}_2\text{O}_3$  content by FactSage.

explain the reason why  $\text{Fe}_2\text{O}_3$  has little effect on the SBT and AFTs and illustrate the behavior of  $\text{Fe}_2\text{O}_3$  during roasting. Because there is 5.93%  $\text{Fe}_2\text{O}_3$  in the stone coal, for the stone coal with 3% and 18%  $\text{Fe}_2\text{O}_3$  addition, the  $\text{Fe}_2\text{O}_3$  content in the blend is actually 8.7% and 20.3%, respectively. As shown in Figure 7, in the  $\text{Fe}_2\text{O}_3$  content ranging from 8.7% to 20.3%, the phase distribution has almost no change, except the hematite content gradually increases. It is inferred that the  $\text{Fe}_2\text{O}_3$  added to the stone coal does not react with others. This is the reason why the  $\text{Fe}_2\text{O}_3$  has little effect on the SBT and AFTs. However, when the  $\text{Fe}_2\text{O}_3$  content is less than 3%, as shown in Figure 7, the  $\text{Fe}_2\text{O}_3$  would react with anorthite to generate andradite and a little amorphous phase. Hence, it is concluded that the  $\text{Fe}_2\text{O}_3$  can stably exist as hematite in the system and does not

react with others, therefore the  $\text{Fe}_2\text{O}_3$  content always has little effect on the sintering during roasting, except for the stone coal with very low  $\text{Fe}_2\text{O}_3$  content (<3%).

**3.3. Effect of  $\text{SiO}_2$  on Sintering Behavior.** The apparent density of roasted samples, plotted as a function of roasting temperature with different  $\text{SiO}_2$  addition content, is provided in Figure 8. Observations from Figure 8 indicate that the SBTs for

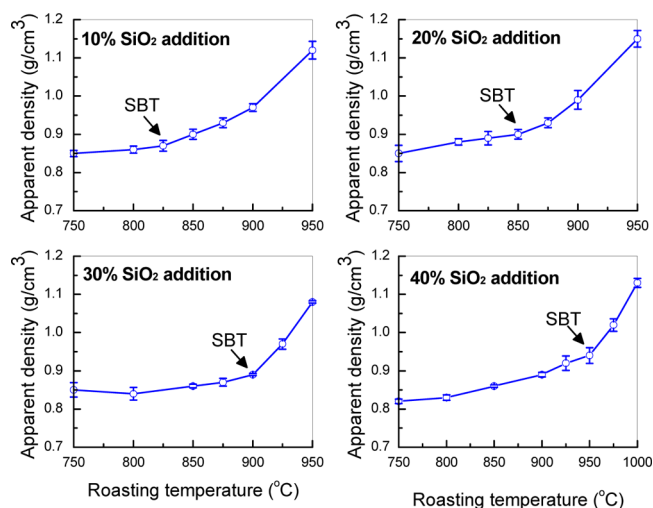


Figure 8. Apparent density against roasting temperature with different  $\text{SiO}_2$  addition contents.

samples with 10%, 20%, 30%, and 40%  $\text{SiO}_2$  addition are 825, 850, 900, and 950 °C, respectively. The SBT increases as the  $\text{SiO}_2$  addition content increases, especially for  $\text{SiO}_2$  addition contents of >20% (Figure 2). The AFTs also increase as the  $\text{SiO}_2$  addition content increases, although the increasing rate of AFTs is slower than that of SBT (Figure 9).

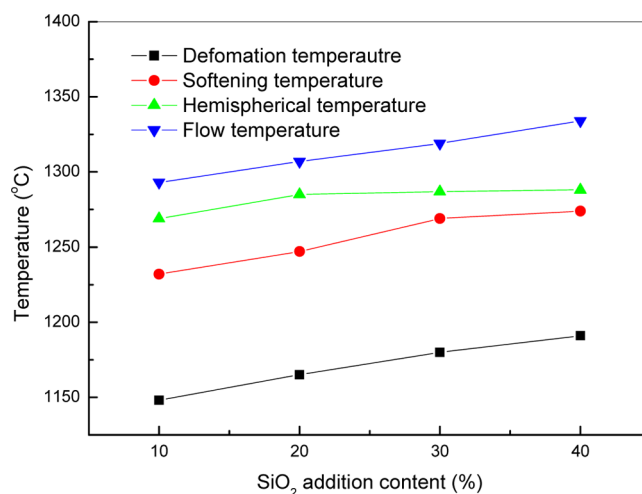


Figure 9. Effect of  $\text{SiO}_2$  addition content on AFTs.

Figure 10 gives the phase distribution for the roasted samples with different  $\text{SiO}_2$  content. Considering the stone coal has 54.36%  $\text{SiO}_2$ , for the stone coal with 10% and 40%  $\text{SiO}_2$  addition, the  $\text{SiO}_2$  content in the blend is actually 58.5% and 67.4%, respectively. As shown in Figure 10a, in the  $\text{SiO}_2$  content range of 58.5%–67.4%, the quartz content increased as other phases content gradually decreased. It is inferred that the  $\text{SiO}_2$  (quartz) added to the stone coal does not react with



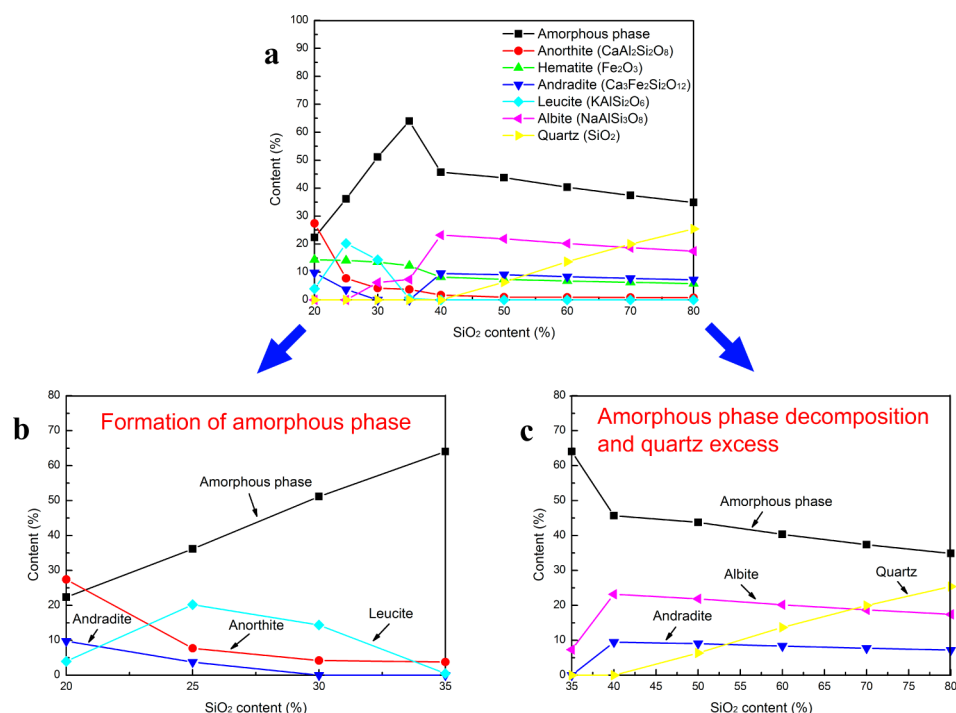


Figure 10. Phase distribution and reaction behavior as a function of SiO<sub>2</sub> content calculated by FactSage.

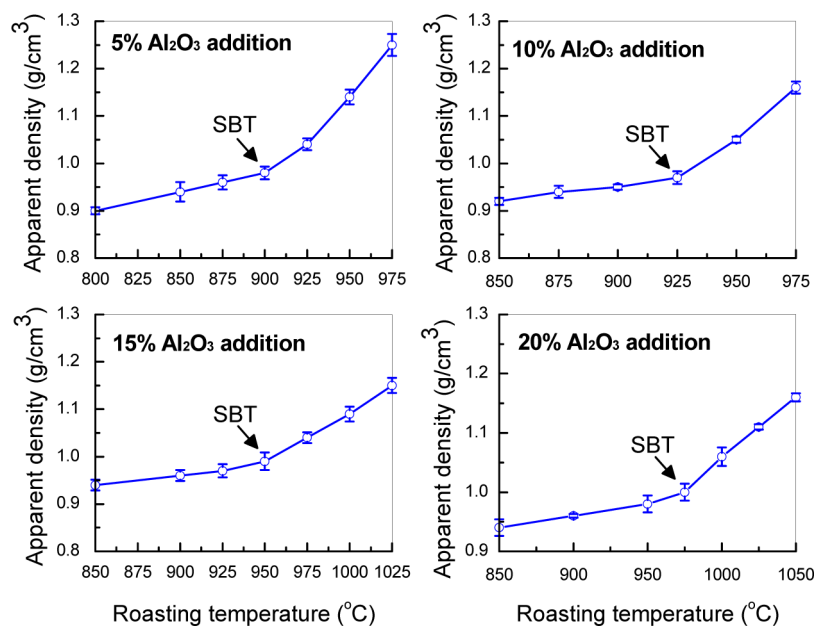


Figure 11. SBTs of samples with different Al<sub>2</sub>O<sub>3</sub> content during roasting.

other phases. The increase in SBT and AFTs with increasing SiO<sub>2</sub> is caused by the excess of quartz, whose melting point is relatively high. In the SiO<sub>2</sub> content range of 20%–35%, it is observed that, with increasing SiO<sub>2</sub> content, the anorthite, andradite, and leucite contents decrease, while the amorphous phase content increases significantly (see Figure 10b). It is inferred that the amorphous phase is generated from anorthite, andradite, and leucite, and quartz also takes part in the reaction for the generation of amorphous phase. However, when the SiO<sub>2</sub> content is in the range of 35%–40%, the amorphous phase content decreases and the albite and andradite contents increase (Figure 10c). It indicates that the amorphous phase

reacts with quartz to generate albite and andradite. It is concluded that, for stone coal with low SiO<sub>2</sub> content (<35%), quartz reacts with anorthite, andradite, and leucite to form an amorphous phase, which easily causes sintering during roasting, whereas, for stone coal with high SiO<sub>2</sub> content (>40%), SiO<sub>2</sub> is excess, which results in relatively high SBT. In fact, the SiO<sub>2</sub> content in decarbonized stone coal is always higher than 40%. Hence, the SiO<sub>2</sub> in stone coal is beneficial to avoid the sintering during roasting.

**3.4. Effect of Al<sub>2</sub>O<sub>3</sub> on Sintering Behavior.** The apparent density of roasted samples, plotted as a function of roasting temperature with different Al<sub>2</sub>O<sub>3</sub> addition content, is provided

in Figure 11. The SBTs for samples with 5%, 10%, 15%, and 20%  $\text{Al}_2\text{O}_3$  addition content are 900, 925, 950, and 975  $^{\circ}\text{C}$ , respectively (Figure 11). The SBT increases directly as the  $\text{Al}_2\text{O}_3$  addition content increases (Figure 2). The AFTs increase as the  $\text{Al}_2\text{O}_3$  addition content increases, which is consistent with the change trend of SBT with increasing  $\text{Al}_2\text{O}_3$  addition content (see Figure 12).

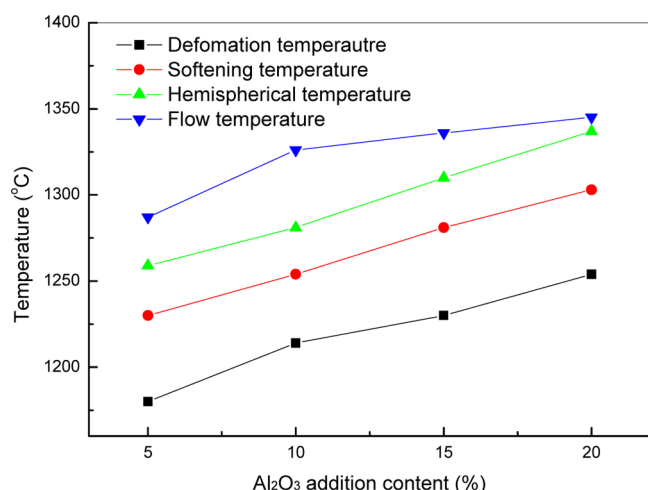


Figure 12. Effect of  $\text{Al}_2\text{O}_3$  addition content on AFTs.

The phase distributions for the roasted samples with different  $\text{Al}_2\text{O}_3$  content are calculated by FactSage to explain the reason why the SBT and AFTs increased as the  $\text{Al}_2\text{O}_3$  addition content increased (see Figure 13). Because the initial stone coal has 10.59%  $\text{Al}_2\text{O}_3$ , for the stone coal with 5% and 20%  $\text{Al}_2\text{O}_3$  addition, the  $\text{Al}_2\text{O}_3$  content in the blend is actually 14.8% and 25.5%, respectively. From Figure 13a, it can be seen that, in the  $\text{Al}_2\text{O}_3$  content range of 14.8%–25.5%, the amorphous phase

proportion decreases linearly until the amorphous phase disappears. In this range, with increasing  $\text{Al}_2\text{O}_3$  content, the amorphous phase gradually decomposes. This also means that the formation of the amorphous phase become difficult, which may account for the fact that the SBT and AFTs in the experiment increased quickly as the  $\text{Al}_2\text{O}_3$  content increased. Also, as shown in Figure 13c, with the decomposition of amorphous phase, the albite and leucite contents increase. It is inferred that the amorphous phase is converted to albite and leucite. For  $\text{Al}_2\text{O}_3$  contents in the range of 22.5%–30%, observations indicate that mullite with a high melting point is generated, which would improve the SBT significantly during roasting (Figure 13b). It is concluded that  $\text{Al}_2\text{O}_3$  in the stone coal is helpful to avoid sintering during roasting, especially for high  $\text{Al}_2\text{O}_3$  stone coal, in which mullite is generated.

#### 4. CONCLUSIONS

With increasing CaO content, the sintering beginning temperature (SBT) and ash fusion temperatures (AFTs) first decrease and then increase during the roasting of stone coal. The behavior of CaO is dependent on its content in stone coal. For stone coal with low CaO content, CaO reacts with albite, leucite, and quartz to generate amorphous phase, which easily causes sintering, while for stone coal with high CaO content, CaO takes part in the formation of andradite and  $\text{Na}_2\text{Ca}_3\text{Si}_6\text{O}_{16}$ . The change of  $\text{Fe}_2\text{O}_3$  content in stone coal has almost no effect on the SBT and AFTs.  $\text{Fe}_2\text{O}_3$  in roasted stone coal always exists stably as hematite in the system and does not react with other compounds. When the  $\text{SiO}_2$  content in stone coal is <35%, quartz reacts with anorthite, andradite, and leucite to form an amorphous phase, which would result in sintering during roasting. For the stone coal with high  $\text{SiO}_2$  content (>40%), the amorphous phase decomposes and quartz is present in excess, and the SBT and AFT values are relatively high. The  $\text{SiO}_2$  content in the decarbonized stone coal is always

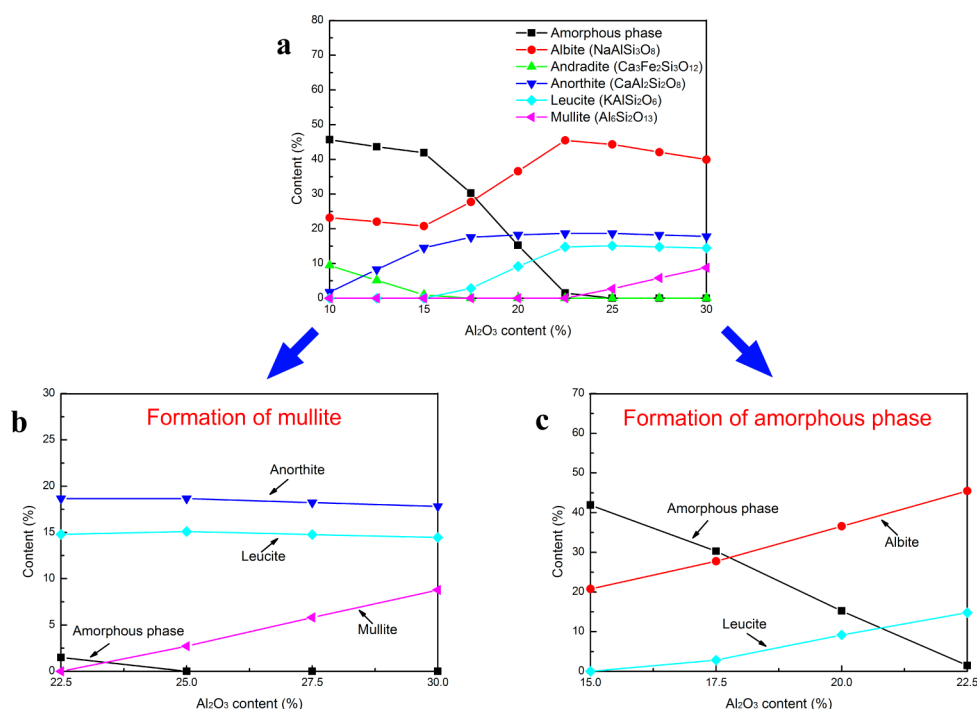


Figure 13. Phase distribution and reaction behavior as a function of  $\text{Al}_2\text{O}_3$  content calculated by FactSage.

higher than 40%; hence, the  $\text{SiO}_2$ , to some extent, is beneficial to avoid sintering during the roasting. The SBT and AFTs increase linearly as the  $\text{Al}_2\text{O}_3$  content increases.  $\text{Al}_2\text{O}_3$  in the stone coal is helpful to avoid sintering during roasting, especially for high  $\text{Al}_2\text{O}_3$  stone coal, in which mullite is generated.

## AUTHOR INFORMATION

### Corresponding Author

\*Tel./Fax: +86 027 87212127. E-mail: zym126135@126.com.

### Notes

The authors declare no competing financial interest.

## ACKNOWLEDGMENTS

This research was supported by the Ministry of Science and Technology of the People's Republic of China (Projects from Key Projects in the National Science & Technology Pillar Program during the Twelfth Five-Year Plan Period, Nos. 2011BAB05B01 and 2011BA05B04) and the Ministry of Education (No. 20120143120007). Appreciation is expressed to Professor J. Han, from Hubei Province Key Laboratory of Coal Conversion and New Carbon Materials, for providing FactSage software.

## REFERENCES

- (1) Zhang, Y.; Bao, S.; Liu, T.; Chen, T.; Huang, J. The technology of extracting vanadium from stone coal in China: History, current status and future prospects. *Hydrometallurgy* **2011**, *109*, 116–124.
- (2) Liu, Y.; Yang, C.; Li, P.; Li, S. A new process of extracting vanadium from stone coal. *Int. J. Min. Met. Mater.* **2010**, *17*, 381–388.
- (3) Wang, M.; Wang, X.; Shen, J.; Wu, R. Extraction of vanadium from stone coal by modified salt-roasting process. *J. Cent. South. Univ. Technol.* **2011**, *18*, 1940–1944.
- (4) Ye, P.; Wang, X.; Wang, M.; Fan, Y.; Xiang, X. Recovery of vanadium from stone coal acid leaching solution by coprecipitation, alkaline roasting and water leaching. *Hydrometallurgy* **2012**, *117*, 108–115.
- (5) Zhu, X.; Zhang, Y.; Huang, J.; Liu, T.; Wang, Y. A kinetics study of multi-stage counter-current circulation acid leaching of vanadium from stone coal. *Int. J. Miner. Process.* **2012**, *114*, 1–6.
- (6) Wang, M.; Xiang, X.; Zhang, L.; Xiao, L. S. Effect of vanadium occurrence state on the choice of extracting vanadium technology from stone coal. *Rare Met.* **2008**, *27*, 112–115.
- (7) Zhao, Y.; Zhang, Y.; Liu, T.; Chen, T.; Bian, Y.; Bao, S. Pre-concentration of vanadium from stone coal by gravity separation. *Int. J. Miner. Process.* **2013**, *121*, 1–5.
- (8) Hu, Y.; Zhang, Y.; Bao, S.; Liu, T. Effect of the mineral phase and valence of vanadium on vanadium extraction from stone coal. *Int. J. Miner. Met. Mater.* **2012**, *19*, 893–897.
- (9) Zhang, Y.; Hu, Y.; Bao, S. Vanadium emission during roasting of vanadium-bearing stone coal in chlorine. *Miner. Eng.* **2012**, *30*, 95–98.
- (10) Chen, T.; Zhang, Y.; Song, S. Improved extraction of vanadium from a Chinese vanadium-bearing stone coal using a modified roast-leach process. *Asia-Pac. J. Chem. Eng.* **2010**, *5*, 778–784.
- (11) He, D.; Feng, Q.; Zhang, G.; Ou, L.; Lu, Y. An environmentally-friendly technology of vanadium extraction from stone coal. *Miner. Eng.* **2007**, *20*, 1184–1186.
- (12) Li, S.; Yao, Q.; Chi, Y.; Yan, J.; Cen, K. Pilot-scale pyrolysis of scrap tires in a continuous rotary kiln reactor. *Ind. Eng. Chem. Res.* **2004**, *43*, 5133–5145.
- (13) Xu, G.; Wang, R. Sintering of stone coal and the transformation of vanadium in Badu and Xicuan. *Chin. J. Rare Met.* **1994**, *18*, 422–427.
- (14) Lu, M.; Zhang, Y.; Liu, T.; Yang, D. Sintering action of sodium calcination during extraction vanadium from stone coal. *Chin. J. Rare Met.* **2009**, *33*, 894–897.
- (15) Dyk, J. Understanding the influence of acidic components (Si, Al, and Ti) on ash flow temperature of South African coal sources. *Miner. Eng.* **2006**, 280–286.
- (16) Xiao, W. Mineralogy of stone coal from Shanglin of Guangxi and vanadium extraction with hydrometallurgical process. *Nonferrous Met.* **2007**, *59*, 85–90.
- (17) Zhao, Y.; Zhang, Y.; Bao, S.; Chen, T.; Han, J. Calculation of mineral phase and liquid phase formation temperature during roasting of vanadium-bearing stone coal using FactSage software. *Int. J. Miner. Process.* **2013**, *124*, 150–153.
- (18) Liao, L.; Wu, R. Optimal control of the sintering strain rate of yttria-stabilized zirconia electrolytes for solid oxide fuel cells using a thermal-mechanical analyzer during the sintering process. *Ind. Eng. Chem. Res.* **2009**, *48*, 7567–7573.